*Present address: Department of Engineering Physics, Research School of Physical Sciences, The Australian National University, Canberra, A.C.T. Australia.
[1]B. A. Kononov and V. K. Struts, Fiz. Tverd. Tela 11, 3577 (1969) [Sov. Phys.-Solid State 11, 2994 (1970)].
[2]M. Mannami, T. Sakurai, K. Ozawa, F. Fujimoto, and K. Komaki, Phys. Status Solidi 38, K1 (1970).
[3]Hj. Matzke, Phys. Status Solidi A 8, 99 (1971).
[4]K. Morita, F. Tachibana, and N. Itoh, Phys. Lett. A 33, 257 (1970).
[5]S. Roth, R. Coutelle, and R. Sizmann, *Atomic Collision Phenomena in Solids*, edited by D. W. Palmer, M. W. Thomson, and P. D. Townsend (North-Holland, Amsterdam, 1970), p. 538.
[6]K. Ozawa, F. Fujimoto, K. Komaki, M. Mannami, and T. Sakurai, Phys. Status Solidi 9, 323 (1972).
[7]E. T. Shipatov and B. A. Kononov, Fiz. Tverd. Tela 10, 854 (1968) [Sov. Phys.-Solid State 10, 670 (1968)].
[8]R. S. Nelson, Philos. Mag. 14, 637 (1966).
[9]J. Lindhard, K. Dan. Vidensk. Selsk. Mat.-Fys. Medd. 34, 14 (1965).
[10]J. A. Davies, J. Denhartog, and J. L. Whitton, Phys. Rev. 165, 345 (1968).
[11]M. J. Hollis, Nucl. Instrum. Methods 103, 337 (1972).
[12]E. Bogh, Can. J. Phys. 46, 653 (1968).
[13]J. U. Andersen, O. Andreasen, J. A. Davies, and E. Uggerhøj, Radiat. Eff. 7, 25 (1971).
[14]Obtained from Harshaw Chemical Co.
[15]Annealing studies showed that all visible color centers were removed after a 10-min anneal at 250 °C and complete recovery of χ_{min} occurred after a 10-min anneal at 400 °C.
[16]L. C. Northcliffe and R. F. Schilling, Nucl. Data A 7, 233 (1970).
[17]D. Pooley and W. A. Runciman, J. Phys. C 3, 1815 (1970).
[18]A. E. Hughes, D. Pooley, H. U. Rahman, and W. A. Runciman, Report No. AERE-R 5604, 1967 (unpublished).
[19]J. H. Schulman and W. D. Compton, *Colour Centres in Solids* (Pergamon, London, 1962).
[20]K. Izumi, J. Phys. Soc. Jap. 26, 1451 (1969).
[21]J. H. Barrett, Phys. Rev. B 3, 1527 (1971).
[22]M. R. Altman, L. C. Feldman, and W. M. Gibson, Phys. Rev. Lett. 24, 464 (1970).

PHYSICAL REVIEW B VOLUME 8, NUMBER 3 1 AUGUST 1973

Multiple Scattering and Planar Dechanneling in Silicon and Germanium

L. C. Feldman
Bell Laboratories, Murray Hill, New Jersey 07974

B. R. Appleton
Oak Ridge National Laboratory, Oak Ridge, Tennessee 37830
and Bell Laboratories, Murray Hill, New Jersey 07974

(Received 24 May 1972)

The dechanneling of MeV protons from the planar channels of silicon and germanium is investigated. The backscattering technique and transmission technique for measuring the dechanneling rate are compared and show good agreement. The data are treated in the framework of a diffusion model which describes the observed energy dependence of the dechanneling length. Various physical mechanisms which contribute to the diffusion are discussed and estimated. Direct measurements of the multiple scattering in the channels are compared to estimates of the diffusion constants.

I. INTRODUCTION

When a collimated beam of charged particles is incident parallel to a major symmetry direction in a single crystal, the ions approach the rows or planes of atoms at the crystal surface over a wide range of impact parameters. As the ions are transmitted through the crystal surface, they acquire momenta transverse to the symmetry direction depending upon these initial impact parameters. In the simplest channeling model, when the beam reaches an equilibrium distribution inside the crystal, some of the ions have been deflected through angles greater than the critical angle for channeling, ψ_c, and are said to be in the nonaligned or random beam; and the remainder of the ions are said to be in the aligned or channeled beam. In this approximation the motion of each channeled ion is governed by a potential which is constant in the longitudinal direction and whose magnitude is derived from averaging the atomic potential. Furthermore, since the potential is constant in the longitudinal direction, the channeled fraction would be predicted to be independent of thickness (aside from effects due to the energy loss of the particle as it traverses the crystal) and the ions might be expected to maintain their particular trajectories. In fact, however, a large experimental thickness dependence is observed. The measured critical angles and minimum yields are in reasonable agreement with theory only for channeling in very thin crystals[1] or near the surfaces of thick crystals.[2,3] Initially well-channeled ions acquire higher transverse momenta as they penetrate deeper into the crystal until they "escape" the channel and become part of the random beam. Conversely, initially randomly directed ions undergo multiple scattering and may "infuse" into channeling directions where

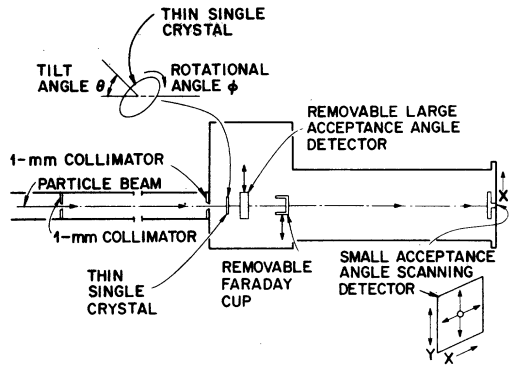

FIG. 1. Schematic of experimental apparatus used in measuring transmitted energy and intensity distributions.

they take on the characteristics of channeled ions.

It is important to understand these so-called "thickness effects" for both fundamental and practical reasons. The physical processes that are responsible for the ultimate escape of an initially well-channeled ion are certainly of interest, and from the practical point of view essentially all measurements are subject to some thickness effects. The channeling and blocking phenomena are being used in more detailed measurements as tools for extracting ion-impanted damage profiles, range distributions, nuclear-lifetime parameters, etc. The better one can interpret the relative importance of escape, the more accurate the information extracted from such measurements will be.

In this study we shall first (i) describe a method of extracting the characteristic thickness parameter by measurement of the transmitted-particle energy spectrum, (ii) compare this method with the more usual backscattering method, and (iii) discuss in detail the conversion of energy to depth necessary in both of the methods in order to obtain the thickness parameter. Measurements of the energy dependence of this parameter will be presented for various planes in Si and Ge. We shall then present measurements of the multiple scattering of the channeled beam and its energy dependence to try to account for the observed decay rates. Finally, a discussion is presented which applies a simple diffusion model to the escape and considers the relative importance of the physical mechanisms which cause this diffusion and hence escape.

This work includes and is an extension of investigations presented at the International Conference on Solid State Physics Research with Accelerators.[4,5] Observations of thickness effect were previously discussed by Andersen *et al.*,[6] Davies *et al.*,[2] and Feldman[1] and predicted by Lindhard.[7] Experiment and theory relating to the multiple scattering of channeled ions were also discussed by Thompson[8] and Dearnaley *et al.*[9] Since that time various authors have considered the problem including Abel *et al.*,[10] Foti and co-workers,[11] Morita and Itoh,[12] and Altman.[13]

II. EXPERIMENTAL METHOD

A. Wide-Acceptance-Angle Measurements

Total energy distributions of ions transmitted through thin single-crystal targets were recorded using a large-active-area solid-state charged-particle detector placed directly behind the crystals. This detector, labeled in Fig. 1 as a removable large-angle detector, accepted all ions with emergence angles $\lesssim 15°$ to the incident beam, and the energy spectra were recorded using a on-line SDS-910 computer programmed as a 512-channel pulse-height analyzer. The signal-handling electronics were standard, and the energy resolution of the detector was 25 keV. The goniometer accuracy and reproducibility along with more specific details of the experimental setup are discussed in an earlier publication.[14]

B. Energy and Angular Distributions of Transmitted Ions

The energies and intensities of ions transmitted through thin single crystals were recorded at selected angles of emergence with the aid of a small-acceptance-angle solid-state scanning detector. All obstacles were removed from the paths of the transmitted ions, and their emergent distributions were recorded in the x-y plane as illustrated in Fig. 1. The detector, which had an acceptance angle of 0.05° and an energy resolution of 25 keV, could be accurately positioned over a wide range of emergence angles.

For a particular crystal orientation intensities at various emergence angles were normalized relative to each other with the aid of a monitor detector placed at large angles to record Rutherford-scattered ions. The electronics of the detecting system and the goniometer were the same as discussed in Sec. II A. The angular divergence of the incident beam was 0.015° half-angle.

C. Large-Angle Rutherford-Scattering Measurements

The yields and energy spectra of ions Rutherford scattered to angles from 170° to 177° were recorded with the aid of an annular solid-state detector employed in the configuration shown schematically in Fig. 2. The acceptance geometry of the annular detector assured that the backscattered ions were averaged over the azimuthal emergence directions. The proton beam collimated to a half-angle of divergence of 0.04°, was backscattered from a thick single-crystal target held in a goniometer arrangement. A shield held at liquid-nitrogen

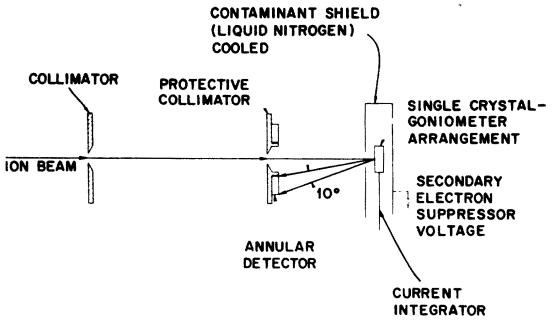

FIG. 2. Experimental arrangement for measuring Rutherford-backscattered yields and energy spectra.

temperatures reduced surface contamination, and secondary-electron emission was reduced by negatively biasing a shield relative to the target. The energy spectra recorded with the annular detector were amplified and recorded using a 512-channel pulse-height analyzer. Various spectra were normalized for the same total charge integrated from the target.

III. RESULTS AND ANALYSIS

A. Measurements of Characteristic Escape Parameters

In a typical planar channeling experiment ~70% of the incident ions are initially channeled, and only ~30% are initially in the random component of the beam. However, as the channeled ions penetrate deeper into the crystal they begin to escape. Their rate of escape can be determined by a number of experimental methods, and some of these techniques are detailed below. Measurements of $x_{1/2}$, the characteristic crystal thickness at which one-half of the initially channeled ions have escaped, are obtained for a number of cases using each method.

1. Total-Transmitted-Energy Distributions

This method for measuring $x_{1/2}$ values uses the total-energy spectrum for ions transmitted through thin single-crystal targets. Such spectra were recorded using the large-acceptance-angle solid-state detector shown in Fig. 1 positioned directly behind the crystal. Figure 3 shows two such energy spectra recorded for 3.0-MeV protons transmitted through a 33-μm-thick silicon single crystal in the {110} and {111} planar-channeling directions. The random energy in these two spectra labeled E_R is just the average energy with which a proton emerges when transmitted through a misoriented single crystal of the same thickness. Such an ion has an average energy-loss rate $\langle dE/dx\rangle_R$ that is the same as that in an amorphous material. The energies marked E_C correspond to those protons which are well-channeled through the entire crystal and have a much lower average energy-loss rate $\langle dE/dx\rangle_C$. The values E_C and E_R were determined for this crystal from separate experimental measurements designed specifically for this purpose. This method is outlined in a previous paper.[14]

The spectrum in the energy region between E_R and E_C results primarily from particles which were initially channeled into the crystal to some depth x, but then escaped and became part of the random beam. It is clear from the spectra that the decrease in this region is approximately exponential so that the energy distribution of the escaped particles has the form

$$N(E) = Ae^{-kE} \quad , \tag{1}$$

where $N(E)$ is the number of particles emerging with energy E in the interval $(E,\ E+dE)$ from the crystal, A is an arbitrary constant, and k is the constant of physical interest which is related to $x_{1/2}$.

We can relate the measured energy of the transmitted protons to the distance x into the crystal where they escaped the channel as follows: Consider a proton of incident energy E_I which is initially channeled but that escapes the channel at a distance x into the crystal and traverses the remaining crystal thickness, $(t-x)$, as a "random ion." The emerging ion will have an energy E given by

$$E = E_I - \int_0^x \left(\frac{dE}{dx}\right)_C dx - \int_x^t \left(\frac{dE}{dx}\right)_R dx \quad , \tag{2}$$

where $(dE/dx)_C$ and $(dE/dx)_R$ are the stopping powers for the channeled and "random" ions, respectively. Normally, both stopping power expressions are functions of the energy and change as the protons lose energy, but in transmission measurements through thin crystals such as these where the protons lose less than 25% of their energy, one can replace the integrals in Eq. (2) with average dE/dx values taken at an appropriate intermediate energy, i.e.,

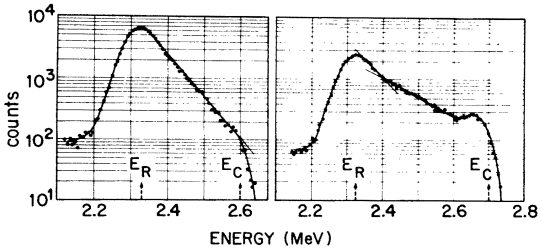

FIG. 3. Total energy distributions for 3.0-MeV protons transmitted parallel to the {110} planes (left-hand spectrum) and {111} planes (right-hand spectrum) of a 33-μm silicon single crystal.

TABLE I. Half-thicknesses for escape obtained using the transmission method.

E (MeV)	t (μm)	$x_{1/2}$ (μm)	Crystal orientation
1.3	20	3.1	
1.3	14	2.8	
2.8	33	4.9	
4.9	16	8.5	{110} planes
4.9	33	9.3	silicon
4.8	46	9.7	$R_T\{110\}=0.6$
4.8	50	9.0	
6.9	33	13.5	
6.9	50	12.5	
8.9	33	16.6	
1.3	14	4.0	
2.8	33	8.3	
4.8	47	13.3	{111} planes
4.8	46	14.3	silicon
8.9	46	25.6	$R_T\{111\}=0.44$
8.9	46	25.1	
2.8	23	4.7	
2.8	25	4.8	
4.8	23	8.0	{110} planes
4.8	25	8.0	germanium
6.9	25	9.7	$R_T\{110\}=0.46$
6.9	23	9.65	
8.9	25	14.5	
2.8	25	8.8	{111} planes
4.8	25	11.5–13	germanium
6.9	25	10.8	$R_T\{111\}=0.33$

$$E = E_I - \left\langle \frac{dE}{dx} \right\rangle_C x - \left\langle \frac{dE}{dx} \right\rangle_R (t-x)$$

$$= E_0 + \left\langle \frac{dE}{dx} \right\rangle_R (1-R_T)x \ , \qquad (3)$$

where $E_0 = E_I - \langle dE/dx \rangle_R t$ and

$$R_T = \left\langle \frac{dE}{dx} \right\rangle_C \Big/ \left\langle \frac{dE}{dx} \right\rangle_R \ .$$

Utilizing the observed exponential rate of escape, Eq. (1), and the relationship between observed energy and depth, Eq. (3), we can write for the number of particles that are channeled at a distance x into the crystal,

$$N(x) = (A/k) \exp\left[-k \left(E_0 + \left\langle \frac{dE}{dx} \right\rangle_R (1-R_T)x \right) \right] \ . \qquad (4)$$

Then the half-thickness of escape $x_{1/2}$ is given by

$$x_{1/2} = 0.693/k \left\langle \frac{dE}{dx} \right\rangle_R (1-R_T) \ . \qquad (5)$$

The quantity k is obtained from the slope of the escape portions of the measured energy spectra and R_T is determined from least-energy-loss measurements.[14] The ratios of the channeled to normal energy loss used in the data reported here are listed in Table I. Listed in the same table are the $x_{1/2}$ values for escape of protons for the {110} and {111} planes of silicon and germanium versus the average energy of the channeled ions. Extraction of $x_{1/2}$ values for the {111}-type channels may be complicated by the geometry of the planes of atoms that make up the walls of this particular plane. There are actually two types of planar channels with 0.78- and 2.35-Å separation in this direction with the same planar densities. There is some evidence in the {111} spectrum of Fig. 3 of two distinct slopes, but we have assumed that the most prominent slope which gives the larger $x_{1/2}$ values is the one characteristic of escape from the {111} channels.

A plot of the various $x_{1/2}$ values obtained by the transmission method for silicon and germanium is shown in Fig. 4. A linear dependence of $x_{1/2}$ on energy is seen for both planar channels in silicon, and a similar dependence is observed for germanium and tungsten.[2] This, as well as other observed trends for escaped particles, is explained on the basis of the escape model discussed in Sec. IV of this paper.

It should be mentioned that the values of R_T used in the analysis of these transmission data are those characteristic of the best channeled ions. We

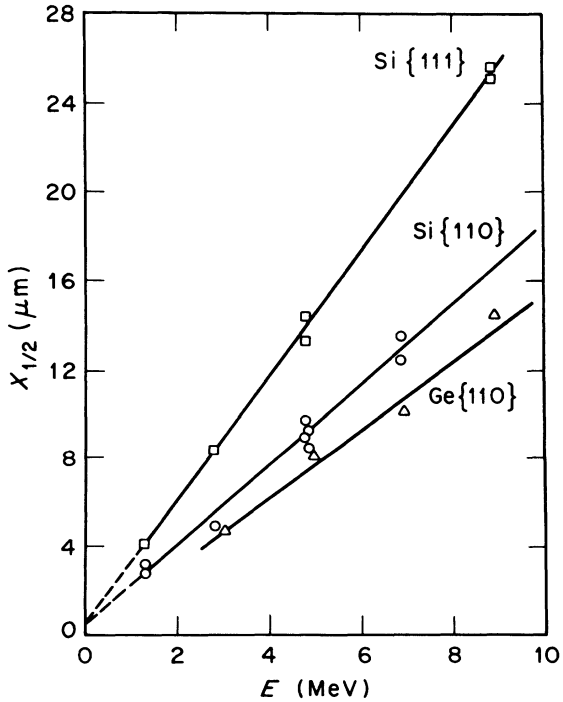

FIG. 4. Half-thickness for escape ($x_{1/2}$) of protons from the {110} and {111} planar channels of silicon as a function of the average energy of the transmitted ions (E).

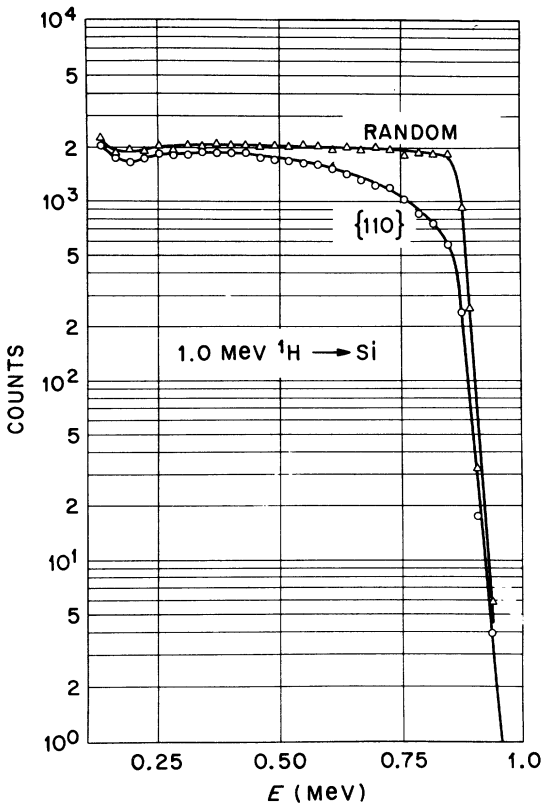

FIG. 5. Energy spectra for 1.0-MeV protons Rutherford backscattered to ~175° from a silicon single crystal oriented with the beam incident in a random direction (Δ) and parallel to the {110} planar direction (○). The two spectra were obtained for the same number of incident protons.

know in fact (Sec. III A 2) that many of the channeled ions have other trajectories and higher-energy-loss rates in the channel,[15] and so we might expect that the average channeled energy loss would have a higher value of R_T. This is discussed in more detail in Sec. III A 3.

2. *Large-Angle Rutherford-Scattering Technique*

Since the majority of channeled ions never approach closer than ~10^{-9} cm to atoms on normal lattice sites, the yield of close-impact-parameter events such as Rutherford elastic scattering or nuclear reactions is reduced. Thus, in a channeling configuration the reaction yield at any depth will be largely dependent on the random fraction of the beam at that depth and one can use this as a sensor of the escape mechanism.

We have used the Rutherford large-angle-scattering technique to detect the random fraction of initially channeled ions as a function of depth for protons in silicon. Two representative energy spectra for 1.0-MeV protons scattered to ~180° from a silicon single crystal are shown in Fig. 5. These spectra were recorded for the same number of protons incident in a random direction and parallel to a {110}-type planar-channeling direction. These plots represent the scattering yield per unit energy (ordinate) as a function of energy (abscissa) where decreasing energy corresponds to particles which have scattered from increasing depths into the crystal. The threshold in the scattering yield that appears at energies ~0.87 MeV corresponds to 1.0-MeV protons that have backscattered from the surface atoms of the silicon crystal and their energy is given by

$$E_0 = E_I\left(1 - \frac{4m_1m_2}{(m_1+m_2)^2}\sin^2\frac{\theta_{c.m.}}{2}\right) = E_I(1-k_s)\ , \tag{6}$$

where E_I is the incident proton energy, m_1 is the proton mass, m_2 is the silicon mass, and $\theta_{c.m.}$ is the center-of-mass scattering angle.

The scattering yield in the {110} spectrum near this threshold is a minimum and is $\chi_m \simeq 0.30$ of the random yield. This minimum yield is in satisfactory agreement with the usual channeling theories which do not include thickness effects. However, such descriptions of the channeling phenomenon would predict that the scattering yield would remain constant at the fraction χ_m for all thicknesses, while it is clear from Fig. 5 that the yield for {110} incidence increases rather rapidly with increasing thickness. This increase in yield is primarily a result of the increase in the random fraction of the beam with increasing penetration into the crystal as a result of proton escape from the channels, and it is this information we wish to extract. There is, however, an additional variation in the scattering yield with energy which results from the energy dependence of the Rutherford-scattering cross section and the stopping-power function for the ions. Such variations can be important, particularly near elastic scattering resonances.

The effect of this energy dependence on extracting escape parameters from the measured channeling spectra can be reduced by obtaining the fraction of the ions in the random component of the beam at each energy, $\chi(E)$; in this way variations in the random and channeled yields due to energy tend to compensate. To be rigorously correct one should take the ratios of the yields at the same thickness instead of the same energy. It is possible to show, however, that the difference between the energy in the channeled spectrum corresponding to scattering from a particlular thickness x and the corresponding energy in the random spectrum is negligible compared to the energy resolution of our system for thicknesses near the crystal surface. Thus, since our analysis is always con-

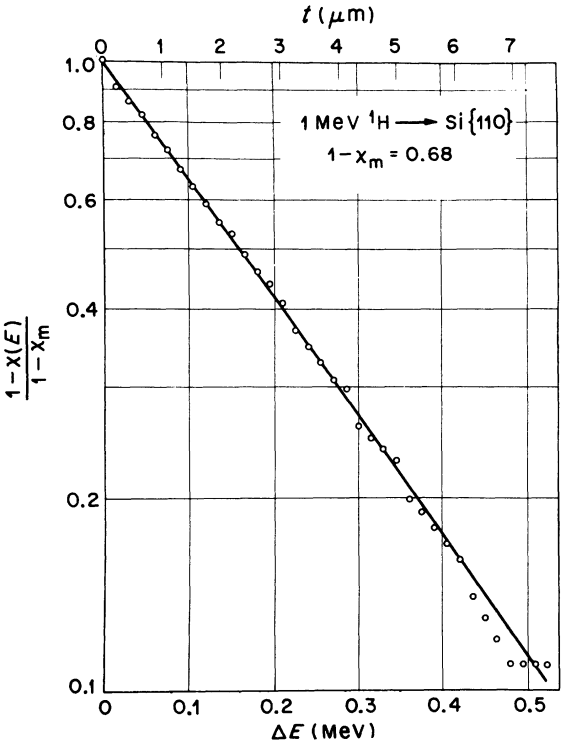

FIG. 6. Fraction of channeled ions, $1-\chi(E)$, relative to the fraction initially channeled, $1-\chi_m$, as a function of observed energy difference ΔE.

fined to thicknesses $\lesssim x_{1/2}$ it is essentially correct to take the ratios of the yields at a particular energy, $\chi(E)$, as being representative of the ratios at a particular thickness, $\chi(x)$. The results of such an analysis are shown in Fig. 6 for the case of 1.0-MeV protons incident parallel to the {110}-type channels of a silicon single crystal. This figure shows the fraction of the proton beam that is channeled at each energy, $1-\chi(E)$, relative to the fraction initially channeled, $1-\chi_m$, as a function of ΔE, where

$$\Delta E = E_0 - E \quad . \tag{7}$$

This semilog plot indicates that the decrease in the channeled fraction of the incident proton beam with energy is approximately exponential, i.e.,

$$(1-\chi(E)) = (1-\chi_m)e^{-K\Delta E} \quad . \tag{8}$$

At large ΔE (corresponding to large x) the data points begin to drop below the straight line which fits the data well at small ΔE. This may be a result of the difference between the energy corresponding to a given thickness for the random and channeled cases mentioned earlier. The exponential dependence seen here for planar channeling has been observed by a number of experimenters.[1,2,6]

We are interested in obtaining $x_{1/2}$ values from data such as those in Fig. 6, where $x_{1/2}$ is that characteristic depth into the crystal at which one-half of the initially channeled particles have escaped, that is, where

$$[1-\chi(E_{1/2})] = \tfrac{1}{2}(1-\chi_m) \quad . \tag{9}$$

To do this we need to relate the observed energy of the backscattered protons, E, to the depth x into the crystal at which they escaped the channel and became part of the random beam.

An analysis similar to that used in the transmission work shows that

$$x_{1/2} = 0.693/K\left\langle\frac{dE}{dX}\right\rangle_R [R_B(1-k_s)+1] \quad , \tag{10}$$

where $R_B = \langle dE/dx\rangle_C / \langle dE/dx\rangle_R$ for the backscattering results. Equation (10) makes use of the fact that the change in the height on the normalized channeling spectrum, ΔN, over a small energy interval ΔE, corresponds to the change in the number of channeled particles in traversing ΔE. Thus for an exponential decay the half-thickness is given by Eq. (10). Note that it is not necessary to make any assumption concerning the depth of dechanneling or the depth of scattering.

The quantity K was determined from the slope of plots of the data like that in Fig. 6, and $\langle dE/dx\rangle_R$ was chosen for each measurement using published energy-loss data.[16] Determination of a value for R_B implies that one knows the average energy-loss-rate distribution for ions which escape and then backscatter. The values obtained for the ratio of channeled to random energy loss from least-energy-loss measurements R_T (those used in Sec. III A1) represent a lower limit to the actual value. It is possible to obtain an estimate for what is probably *an upper limit* by utilizing the elastic scattering resonance that occurs for protons in silicon at a resonance energy of $E_P = 1.65$ MeV. By using an incident energy of 2.0 MeV this resonance samples protons which have escaped at depths several times the half-thickness. Such protons probably diffuse into trajectories with large transverse momenta in the channel before they escape and may experience larger average energy-loss rates.

Two spectra are shown in Fig. 7 for scattering to ~180° of 2.0-MeV protons incident in a random and {110} direction of a silicon single crystal. These spectra appear as standard Rutherford-backscattering spectra except for the characteristic resonance shape which is a result of the 1.65-MeV elastic scattering resonance. First consider the random spectrum. Protons enter the crystal in a random direction at energies $E_I = 2.0$ MeV, lose energy at a rate $\langle dE/dx\rangle_{R,i}$ over a distance Δx_R until they reach the resonance energy $E_\rho = 1.65$

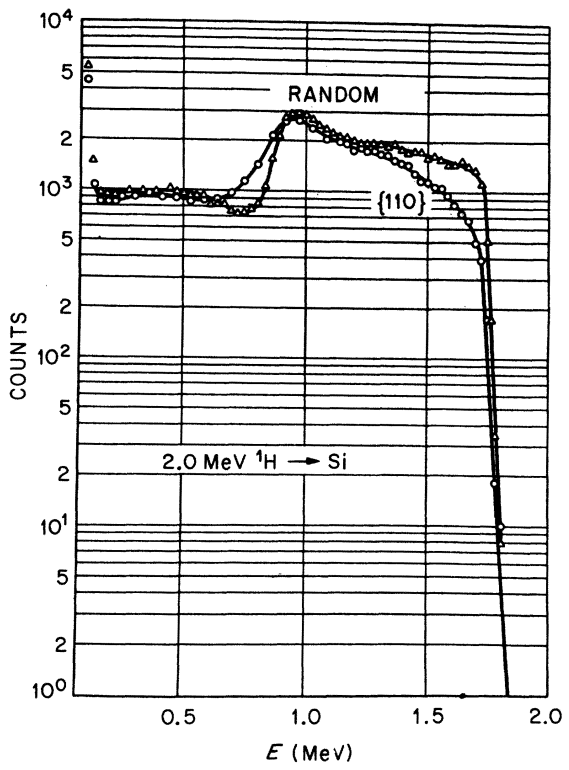

FIG. 7. Normalized energy spectra for 2.0-MeV protons scattered ~175° from a randomly oriented (Δ) and {110} oriented (○) silicon single crystal. The structure at ~0.85 MeV arises from the proton-elastic-scattering resonance in silicon at E_ρ=1.65 MeV.

MeV, undergo resonant scattering, and emerge from the crystal losing energy at the rate $\langle dE/dx\rangle_{R,o}$. The protons in the spectrum at energies E_R = 0.86 MeV can be identified as those which have undergone such a history. Thus, we can write

$$E_R = \left(E_I - \left\langle \frac{dE}{dx}\right\rangle_{R,i} \Delta x_R\right)[1-k_s] - \left\langle \frac{dE}{dx}\right\rangle_{R,o} \Delta x_R \quad , \tag{11}$$

and since

$$\Delta x_R = (E_I - E_\rho) \Big/ \left\langle \frac{dE}{dx}\right\rangle_{R,i} ,$$

we can evaluate

$$\left\langle \frac{dE}{dx}\right\rangle_{R,o} \Big/ \left\langle \frac{dE}{dx}\right\rangle_{R,i} = \frac{E_\rho(1-k_s)E_R}{E_I - E_\rho} \quad . \tag{12}$$

We can do a similar analysis of the {110} channeling spectrum in Fig. 7 and specify that the protons of interest remained in the channel for a distance Δx_C losing energy at the rate $\langle dE/dx\rangle_C = R_B\langle dE/dx\rangle_{R,i}$, escaped the channel with the resonance energy E_ρ = 1.65 MeV, underwent resonant scattering, emerged losing energy at the rate $\langle dE/dx\rangle_{R,o}$, and were observed at the energy E_C = 0.81 MeV. Then,

$$E_C = \left(E_I - R_B\left\langle \frac{dE}{dx}\right\rangle_{R,i} \Delta x_C\right)(1-k_s) - \left\langle \frac{dE}{dx}\right\rangle_{R,o} \Delta x_C$$

$$= E_\rho(1-k_s) - \left\langle \frac{dE}{dx}\right\rangle_{R,o} \Big/ \left\langle \frac{dE}{dx}\right\rangle_{R,I} \frac{E_I - E_\rho}{R_B} \quad , \tag{13}$$

since

$$\Delta x_C = (E_I - E_\rho)/R_B\left\langle \frac{dE}{dx}\right\rangle_{R,i} .$$

Using the value for

$$\left\langle \frac{dE}{dx}\right\rangle_{R,o} \Big/ \left\langle \frac{dE}{dx}\right\rangle_{R,I} = 1.4$$

evaluated from the random spectrum, we find from the equation above that

$$R_B = \left\langle \frac{dE}{dx}\right\rangle_{R,o} \Big/ \left\langle \frac{dE}{dx}\right\rangle_{R,i} \left(\frac{E_I - E_\rho}{E_\rho(1-k_s) - E_C}\right)$$

$$\simeq 0.87 \tag{14}$$

for the {110}-type planar channel. A similar analysis for the {111} planes yielded a value $R_B \simeq 0.81$. These results indicate that those protons which remain in the channel to a depth $\sim\Delta x_C \simeq 14$ μm have an average energy-loss rate in the channel which is ~0.8–0.9 of the average random energy-loss rate. These values, which are considerably larger than the R_T = 0.44 and R_T = 0.6 values measured for best-channeled protons in the {111} and {110} planar channels, respectively, might be expected on the basis of the past history of the ions before escape. Protons which escape at such large depths in the crystal must have had channeled trajectories which approached very close to the atoms which made up the channel walls and would thus have higher-energy-loss rates than best-channeled ions. One could, in fact, use this resonance method to measure R_B as a function of depth for channeled ions. By varying the incident proton energy one could vary the depth Δx_C at which the ions escaped the channel with the resonance energy E_ρ.

Measurements were made using the large-angle Rutherford-scattering technique and the analysis method just outlined for 0.5–2.0-MeV protons in silicon, and the half-thickness values obtained are shown in Table II. In extracting these parameters we have used two R_B values for each channeling orientation; the values in parentheses assume that the energy-loss rate in the channel is the same as obtained in transmission-type measurements of the least energy loss (see Sec. III A 1) and probably represent a lower limit to the actual value of R, while the values for R_B = 0.81 and R_B = 0.87 are close to an upper bound. These $x_{1/2}$ data are plotted in Fig. 8 as a function of E_I. The best straight-line fits to the data do not appear to ex-

TABLE II. Half-thicknesses for escape obtained using the Rutherford-backscattering method.

E_I(MeV)	$x_{1/2}$(μm)	Crystal orientation
0.5	1.2	
	(1.4)	
1.0	2.1	Si {110}
	(2.4)	$R_B = 0.87$
1.5	3.0	($R_B = 0.60$)
	(3.5)	
2.0	3.9	
	(4.5)	
0.5	1.6	
	(2.0)	
1.0	2.7	
	(3.3)	
1.5	3.9	Si {111}
	(4.8)	$R_B = 0.81$
2.0	4.8	($R_B = 0.44$)
	(6.0)	

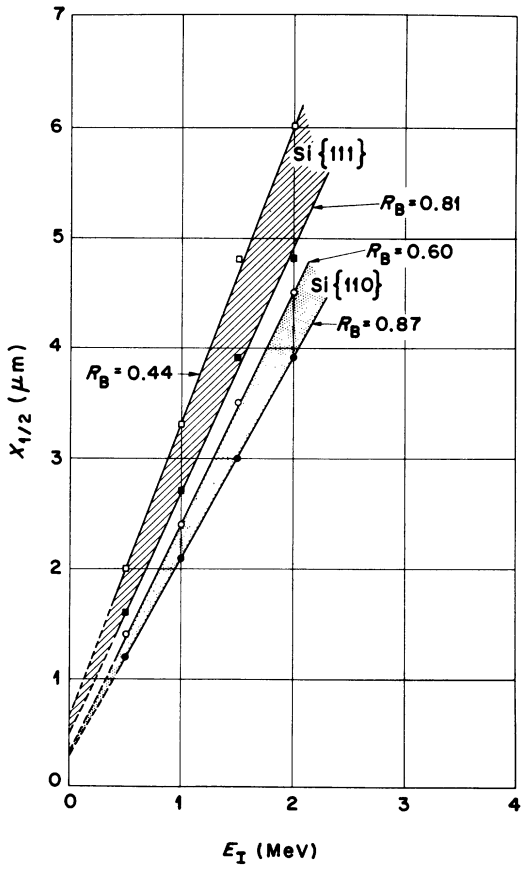

FIG. 8. Half-thickness for escape ($x_{1/2}$) of protons from the {110} and {111} planar channels of silicon as a function of the incident proton energy E_I. These data were obtained using the Rutherford-backscattering technique and analyzed assuming both maximum ($R_B\{110\} = 0.87$, $R_B\{111\} = 0.81$) and minimum ($R_B\{110\} = 0.60$, $R_B\{111\} = 0.44$) estimates of R_B.

trapolate through the origin. A possible explanation for this is offered in Sec. IV. Also, the spread in the data for the two values of R_B indicates the degree of sensitivity of the Rutherford-backscattering method to different choices of R_B.

3. *Comparison of Transmission and Rutherford-Backscattering Method*

Two different methods, the transmission method of Sec. III A1 and the Rutherford-backscattering method of Sec. III A2, have been used to obtain $x_{1/2}$ parameters for the escape of protons from silicon planar channels. An initial comparison of the results of these two methods is shown in Fig. 9. This figure is the same as Fig. 8 (the results of the Rutherford-backscattering method) with the addition of the two dark solid lines which are the best fits to the half-thickness values obtained by the transmission method shown in Fig. 4. Before commenting on the comparison of these results, several points need to be reiterated concerning the two methods.

First of all the two methods have a different sensitivity to the loss rates in the channel (e.g., different R's). The backscattering results are relatively insensitive to the choice of R_B, as Fig. 9

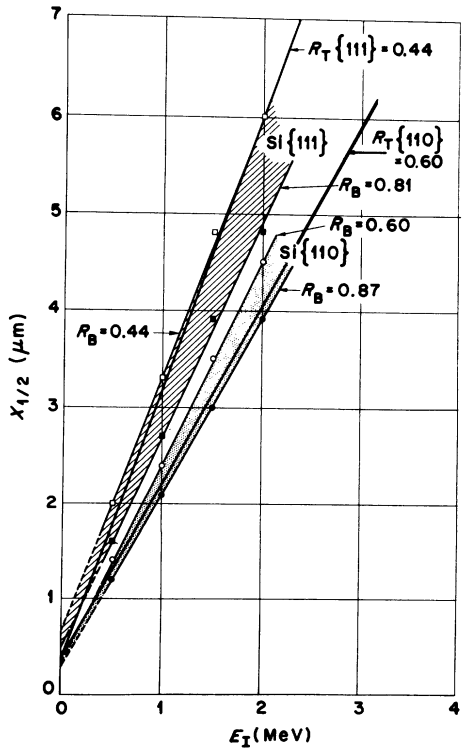

FIG. 9. Comparison of $x_{1/2}$ values obtained by the transmission method (heavy solid lines) and the Rutherford-backscattering method.

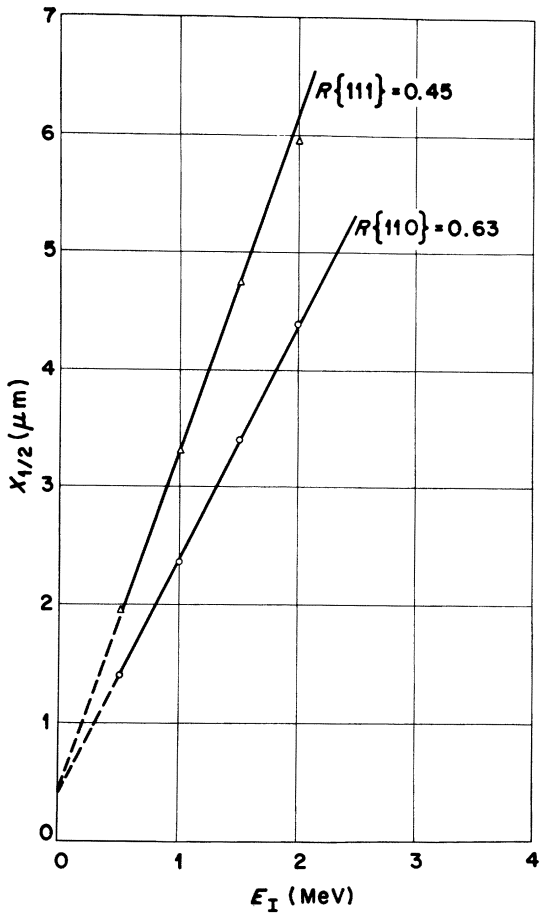

FIG. 10. Comparison between the $x_{1/2}$ values obtained by the transmission method (heavy solid lines) and the Rutherford-backscattering method (data points ○ and △) where the same best-fit values of R are assumed in the analysis, e.g., $R\{110\}=0.63$ and $R\{111\}=0.45$.

shows, while the transmission results are very sensitive to the choice of R_T, so the problem is one of finding the correct value of R_T. One way of confronting this problem is to require that the two methods yield the same $x_{1/2}$ values, treat R as an adjustable parameter, and seek those values of $R=R_B=R_T$ which give best agreement between the transmission and backscattering data. The results of such an approach are shown in Fig. 10 where the solid lines represent the adjusted transmission data and the points the Rutherford-backscattering results. The values of $R_T=R_B$ which give the best agreement are $R\{110\}=0.63$ and $R\{111\}=0.45$. These results are quite reasonable since, as mentioned earlier, the values originally used in interpreting the transmission data, $R_T\{110\}=0.60$ and $R_T\{111\}=0.44$, are probably too low because they were measured for least-energy-loss protons in silicon.[14]

A final point to be made in comparing these methods is illustrated in Fig. 11. Values of $x_{1/2}$ were measured by these two methods on the same sample by using a thin (14-μm) silicon sample and looking at the transmitted energy distributions in a large-solid-state detector (right-hand spectrum) and the Rutherford-backscattering spectra in an annular detector (left-hand spectrum). The $x_{1/2}$ thicknesses obtained by these methods on the same sample agreed with the previous results obtained by the corresponding techniques on a variety of samples.

B. Multiple-Scattering Measurements

We have seen ample evidence in the measurements so far presented that the trajectories of initially well-channeled ions become perturbed with increasing crystal thickness to the point where they eventually escape the channel. As discussed in Sec. IV, the most probable source of this perturbation is multiple scattering of the ions with the electrons in the channels and the atoms that form the channel walls. These multiple scatterings tend to increase the transverse momenta of the ions. This broadening perpendicular to the plane terminates in particle escape once the crossing angle of a particular ion trajectory at the center of a planar channel exceeds the critical angle for channeling. However, trajectories which are perturbed parallel to the planar direction are unconfined, and the resultant mean-square multiple-scattering angle measured in that direction will be characteristic of the multiple-scattering process responsible for the perturbation. This section reports measurements of the multiple-scattering angles which are compared to the escape model in Sec. IV.

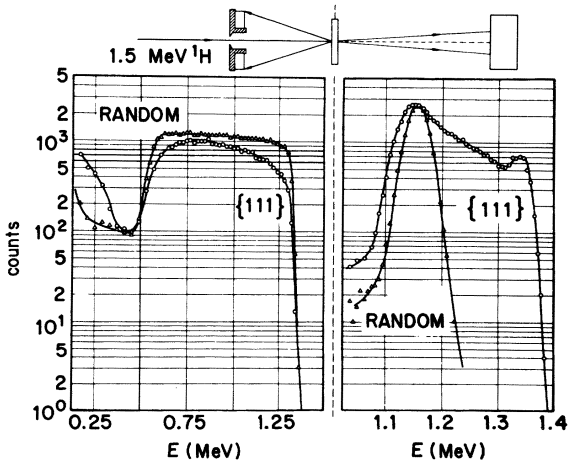

FIG. 11. Comparison of data obtained by Rutherford backscattering (left-hand spectra) and transmission (right-hand spectra) of 1.5-MeV protons on the same thin (14-μm) silicon single crystal.

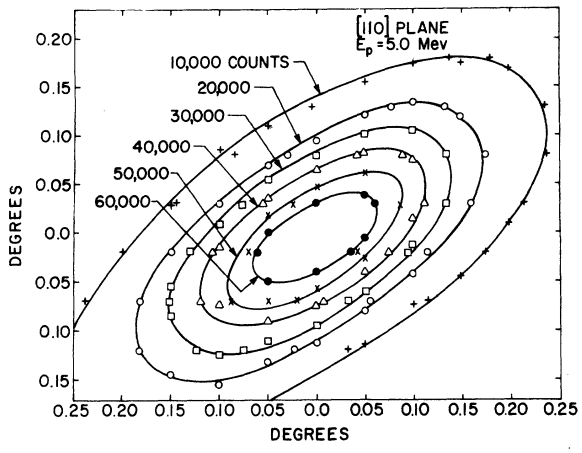

FIG. 12. Intensity contours as a function of emergence angles for 5.0-MeV protons incident parallel to the {110} planar direction of a 33-μm silicon single crystal. Only those protons transmitted with the least energy loss were used.

The results of one such measurement are illustrated in the transmitted proton intensity contour of Fig. 12. A beam of 5.0-MeV protons collimated to a half-angle of divergence 0.015° was transmitted through a 33-μm-thick silicon single crystal parallel to the {110} plane. Using a solid-state charged-particle detector which had an angular resolution of 0.05° and an energy resolution of 25 keV, the entire emergent distribution of the transmitted protons was determined in the manner outlined in Sec. II. To obtain the intensity contour distribution shown in Fig. 12 only those protons which were well channeled (i.e., had the least energy loss) were recorded. This ensured that the distribution is characteristic of only those protons which initially started in the center of the {110} planar channel and remained channeled throughout the crystal thickness. The elongated axis of the contour in Fig. 12 is parallel to the {110} plane. The defining angle perpendicular to the {110} planar direction in the intensity contour is due to the channeling critical angle; any ions whose crossing angle exceed ψ_c will escape the channel and have too high a rate of energy loss to be recorded. A plot of the intensity distribution along the {110} plane can be used to extract an angle characteristic of the multiple-scattering process. Two such intensity plots are shown in Fig. 13 for 9.0- and 3.0-MeV protons transmitted parallel to the {110} planes of a 25-μm-thick germanium crystal. The shapes of the distributions are Gaussian-like, and the mean-square multiple-scattering angles at e^{-1} of the maximum intensity are indicated on the plots. The results of a number of such measurements in various planes of silicon and germanium are displayed in Fig. 14 as a plot of $\langle\theta^2\rangle^{1/2}$ as a function

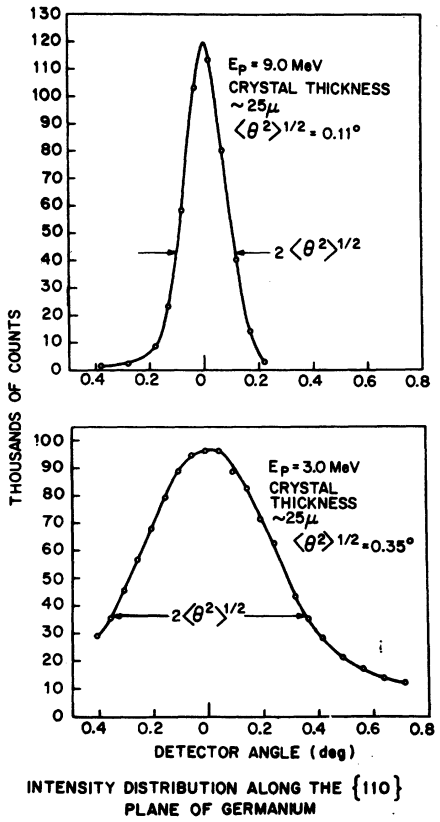

FIG. 13. Two typical emergent intensity distributions taken along the {110} planes of a 25-μm germanium single crystal.

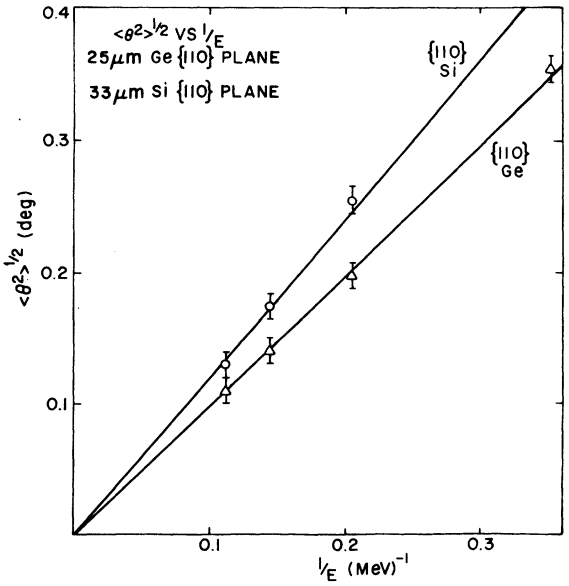

FIG. 14. Measured root-mean-square multiple-scattering angles $\langle\theta^2\rangle^{1/2}$ for scattering along the {110} planes of Si and Ge as a function of energy.

of E^{-1}. This energy dependence as well as the multiple-scattering mechanism is discussed below.

IV. DISCUSSION

A. Diffusion Model

Lindhard[7] has suggested that the observed thickness effects are a result of a multiple-scattering mechanism; a scattering mechanism which gradually increases the crossing angle (e.g., the angles at the midpoint between planes) of the channeled particles and their corresponding transverse energy until the transverse energy is too great for channeling to take place.

We can write down a formalism corresponding to this diffusion by multiple scattering as a guide in treating the data presented in Sec. III. Diffusion theory can be applied to any random-walk process, the physical scattering mechanism being incorporated in the diffusion constant D. Lindhard[7] has previously discussed the problem of escape and the diffusion in crossing angle and has suggested the treatment of the problem in a somewhat different manner.

A general form of the diffusion equation applicable to the multiple-scattering problem may be written

$$\frac{\partial n(\theta_x,\theta_y,t)}{\partial t}=\frac{\partial}{\partial\theta_x}\left(D(\theta_x,\theta_y)\frac{\partial n(\theta_x,\theta_y,t)}{\partial\theta_x}\right)+\frac{\partial}{\partial\theta_y}\left(D(\theta_x,\theta_y)\frac{\partial n(\theta_x,\theta_y,t)}{\partial\theta_y}\right), \quad (15)$$

where $n(\theta_x,\theta_y,t)$ is the distribution function for the particle intensity at the angles $(\theta_x,\ \theta_y)$ at thickness t, and D is the diffusion constant, in general, a function of angle.

In the case of normal multiple Coulomb scattering in an amorphous isotropic solid this diffusion equation and its boundary conditions may be written

$$\frac{\partial n_x(\theta_x,t)}{\partial t}=\frac{D\partial^2 n_x(\theta_x,t)}{\partial^2\theta_x}\ , \quad (16)$$

$$n_x(\infty,t)=n_x(-\infty,t)=0\ , \quad (17)$$

$$n_x(\theta_x,0)=\delta(\theta_x)\ , \quad (18)$$

and similarly for θ_y, where $n(\theta_x,\ \theta_y,t)$ will now be the product solution $n(\theta_x,\theta_y,t)=n_x(\theta_x,t)n_y(\theta_y,t)$ and $\delta(\theta_x)$ is the Dirac δ function.

The well-known solution is the Gaussian

$$n_x(\theta_x,t)=\frac{1}{(4\pi Dt)^{1/2}}e^{-\theta_x^2/4Dt} \quad (19)$$

and represents the solution to the multiple-Coulomb-scattering problem. By assigning $4Dt=\langle\theta^2\rangle$, where $\langle\theta^2\rangle$ is the mean-square multiple-Coulomb-scattering angle, the solutions are put in the more familiar form

$$n(\theta_x,\theta_y,t)=\frac{1}{\pi\langle\theta^2\rangle}\exp\left(\frac{-(\theta_x^2+\theta_y^2)}{\langle\theta^2\rangle}\right)\ . \quad (20)$$

1. Planar Channeling

It is possible to consider multiple scattering for channeled particles in a plane in a similar manner. In general the following differences from the problem described above should be incorporated into the formalism: (i) The diffusion constant may be a function of θ_x and θ_y; (ii) the problem is no longer isotropic, the particles trajectory being confined by the planar walls in the θ_x direction but not confined in the θ_y direction; and (iii) the initial distribution may not be well represented by a δ function.

Unfortunately all of these factors are not easily included in the sophisticated treatment required. Since these diffusion arguments are merely presented as a guide to treating the previously described data, we shall incorporate some of the simpler modifications to the problem. The importance of each of these points will be thoroughly discussed in a later section.

Thus we assume that the diffusion constant is independent of θ_x and θ_y and the initial distribution is given by a δ function. The appropriate diffusion equation and boundary conditions then reduce to

$$\frac{\partial n_x(\theta_x,t)}{\partial t}=\frac{D[\partial^2 n_x(\theta_x,t)]}{\partial\theta_x^2}\ ,$$

$$n_x(\theta_C,t)=n_x(-\theta_C,t)=0\ , \quad (21)$$

$$n_x(\theta_x,0)=\delta(\theta_x-\theta_{x,i})\ ,$$

while the equations for $n_y(\theta_y,t)$ are given by Eqs. (16)–(18). In these equations $n=n_x n_y$ is the distribution function for channeled particles, θ_C is the maximum angle for channeling, $\theta_{x,i}$ is the incident beam direction, and D is the diffusion constant in the channel and not necessarily the same as in the normal multiple scattering problem. [In this paper three symbols are used to represent quantities which are the order of magnitude of the critical angle for channeling. The difference in their use is as follows: (a) ψ_C represents the critical angle for channeling i.e., as measured in a backscattering experiment; (b) ψ_1 represents the combination of constants given by

$$\psi_1=\left(\frac{2Z_1Z_2e^2}{Ed}\right)^{1/2}\ ;$$

(c) θ_C represents the cutoff angle in the diffusion problem. A symbol different than ψ_C is employed since θ_C might easily be used as a fitting parameter in an extension of the work presented here. For quantitative estimates θ_C and ψ_C are interchangeable.] The solutions to this problem are

$$n_x(\theta_x, t) = \sum_{n=1}^{\infty} a_n \sin\left(\frac{n\pi(\theta_x + \theta_C)}{2\theta_C}\right)\exp\left(\frac{-Dn^2\pi^2 t}{4\theta_C^2}\right) , \tag{22}$$

where a_n is given by

$$a_n = \frac{1}{\theta_C}\int_{-\theta_C}^{\theta_C} n(\theta_x, 0)\sin\left(\frac{n\pi(\theta_x + \theta_C)}{2\theta_C}\right)d\theta_x . \tag{23}$$

Integrating, we obtain

$$n_x(\theta_x, t) = \frac{1}{\theta_C}\sum_{n=1}^{\infty}\sin\left(\frac{n\pi(\theta_{x,i} + \theta_C)}{2\theta_C}\right) \times\sin\left(\frac{n\pi(\theta_x + \theta_C)}{2\theta_C}\right)\exp\left(\frac{-Dn^2\pi^2 t}{4\theta_C^2}\right) . \tag{24}$$

The distribution in the angle θ_y is subject to the same boundary equations as the multiple-Coulomb-scattering problem [Eqs. (17) and (18)]. Thus

$$n_y(\theta_y, t) = \frac{1}{(4\pi Dt)^{1/2}} e^{-\theta_y^2/4Dt} . \tag{25}$$

The total number $N(t)$ channeled at thickness t is

$$N(t) = \int_{\theta_y=-\infty}^{\theta_y=\infty} n_y(\theta_y, t)\, d\theta_y \int_{\theta_x=-\theta_C}^{\theta_x=\theta_C} n_x(\theta_x, t)\, d\theta_x \tag{26}$$

or

$$N(t) = \frac{4}{\pi}\sum_{n=0}^{\infty}\cos\left(\frac{(2n+1)\pi\theta_{x,i}}{2\theta_C}\right)\frac{(-1)^n}{2n+1} \times\exp\left(\frac{-D(2n+1)^2\pi^2 t}{4\theta_C^2}\right) . \tag{27}$$

Associating D with the mean-square multiple-scattering angle $\langle\theta^2\rangle_t t$ and treating the case for $\theta_{x,i} = 0$, we obtain

$$N(t) = \frac{4}{\pi}\sum_{n=0}^{\infty}\frac{\exp[-(2n+1)^2\pi^2\langle\theta^2\rangle_t t/16\theta_C^2](-1)^n}{2n+1} , \tag{28}$$

where $4D = \langle\theta^2\rangle_t$.

Equation (28) represents the total number of particles channeled as a function of depth into the crystal. The quantity $N(t)$ may be calculated explicitly with a knowledge of $\langle\theta^2\rangle_t$. An experimental value for this quantity can be determined from the measured distribution along the plane (in the θ_y direction) if the distribution in θ_y can be described by Eq. (26) and if one assumes that the diffusion constant along the plane is the same as across the plane. As will be shown later, the terms with $n > 0$ in the sum are negligible in the valid region of Eq. (28) and thus $N(t)$ may be approximately given by

$$N(t) = (4/\pi)\exp(-\pi^2\langle\theta^2\rangle_t t/16\theta_C^2) , \quad \theta_{x_i} = 0 . \tag{29}$$

The half-thickness $x_{1/2}$ is thus

$$x_{1/2} = \ln 2\,\frac{16\theta_C^2}{\pi^2\langle\theta^2\rangle_t} \cong 1.12\,\frac{\theta_C^2}{\langle\theta^2\rangle_t} . \tag{30}$$

Noting that θ_C^2 is proportional to $1/E$ and $\langle\theta^2\rangle_t$ is proportional to $1/E^2$ (from Fig. 14), we see that

$$x_{1/2} \propto E .$$

Before applying this formalism to the data a few qualifying remarks must be made.

2. *Initial Conditions*

We have taken the initial distribution to be a δ function in angle space. The effect of this is to produce a certain initial depth in which no escape occurs since the particles have not yet acquired angles large enough to bring them close to the planar walls. This effect is actually an artificial one produced by the calculation. Even in the case of perfect collimation, as the beam crosses the crystal surfaces and feels the average potential the channeled component acquires an initial distribution in an angle which populates all angles up to the critical angle. This distribution can easily be calculated using a reasonable planar potential and is approximately given by $n(\theta, 0) = e^{-4\theta^2/\theta_C^2}$. The distribution turns out to be almost Gaussian with a width characteristic of the critical angle. This is very close to the θ distribution calculated in Eq. (24) after the beam has transversed some depth into the crystal, i.e., $t \sim 0.1 x_{1/2}$. Thus we expect the $N(t)$ calculated in Eq. (28) to be valid only at depths greater than $\sim 0.1 x_{1/2}$.

An initial flat (nonexponential) part to the $N(t)$ curve is often observed experimentally as shown in Ref. 2. We believe that this original reduction in the dechanneling rate is due to those particles that have a higher than normal probability of scattering. They are groups that spend an appreciable part of their path in the high density near and in the planes and as a result have a higher Rutherford-scattering probability than normal as well as a high-multiple-scattering probability. The former property adds to the scattering intensity making the channeled fraction appear smaller in the region near the surface. As the beam penetrates, this group is rapidly multiply scattered out of its original directions leaving only the channeled ions with their exponential decay. This effect is of importance[17] in the extraction of the number of particles initially channeled, $N(0)$, in a planar direction. The simple calculation presented here does not take this effect into account.

3. *Diffusion Constant*

In the most general case the diffusion constants applicable in the θ_x and θ_y directions may be different and may each be a function of θ_x, the crossing angle. In the present calculation we have assumed that

$$D(\theta_x, \theta_y) = D ,$$

that is, that the diffusion constant is angle (trajectory) independent and the diffusion constant along the plane is identical to the diffusion constant across the plane. The validity of both of these assumptions rests very heavily on a knowledge of the physical mechanisms.

B. Multiple-Scattering Measurements

The multiple scattering is a result of the interaction of the channeled ions with the electrons and/or screened atoms of the substrate. The multiple scattering of a planar channeled ion can be expected to display some interesting differences from the Coulomb multiple scattering of an ion traversing an amorphous material.

1. Discrete Interactions

In the simplest model of channeling the incident ion is confined to stay within the plane by the average potential and, neglecting the electronic contribution, there is no mechanism for the channeled beam to spread either across the plane or along the plane. In actual fact the potentials are not perfect equipotential planes parallel to the atomic plane but have fluctuations relative to the average value which become less important at large distances from the planes. These fluctuations may give rise to a multiple scattering both along and across the plane and such a mechanism may be important in determining the escape rate. There are not yet any reliable calculations for the "across-the-plane" case. Lindhard[7] has discussed this in the axial case and concludes that it can only give rise to a small-scattering effect.

Estimates of the "along-the-plane case" have been performed by Schiøtt.[18] In this calculation the rate of spreading along the plane is dependent on the transverse energy of the particle, larger transverse energies coming closer to the plane and thus having a larger multiple scattering. For fairly low transverse energies this calculated spreading is a factor of 10 too small to explain the observed spreading shown in Figs. 13 and 14. Comparison with small transverse energies is legitimate in this case since the experimental distributions are of well-channeled particles.

2. Thermal Vibrations

The velocity of MeV protons is much greater than the thermal velocity of ions in a solid and hence the proton sees a stationary lattice with irregularity due to thermal vibrations. Such displacements may be significant contributors to the scattering of channeled particles. Some realistic idea of the effect of the spreading due to nuclear encounters has been calculated by Barrett[19] who includes thermal vibrations and show that, in the absence of electronic multiple scattering, the mean-square angular spread of the beam $\langle\theta^2\rangle_t$ is 1.4×10^{-4} deg$^2/\mu$m, while the measured angular spread is $\sim 2.3\times10^{-3}$ deg$^2/\mu$m. This suggests that the electronic mechanism must also contribute importantly.

3. Multiple Scattering from Interstitials

Displaced lattice atoms and nonsubstitutional impurities may contribute to the dechanneling of the aligned beam. These atoms may contribute to the dechanneling in two ways: (i) by single scattering and (ii) by atomic multiple scattering. In this section we shall estimate the required interstitial densities in order for these mechanisms to play a significant role in the dechanneling process.

It is not difficult to show that for a single scattering process the expected $x_{1/2}$ value is given by

$$x_{1/2}\Big|_{\substack{\text{single}\\ \text{scat.}}} \cong \frac{\ln 2}{\sigma_s n} \simeq \frac{2.8}{\pi}\,\frac{\theta_c^2}{\psi_1^4 d^2 n} \quad ,$$

where n is the interstitial volume density and σ_s is the total Rutherford cross section for scattering to an angle greater than θ_c. For multiple scattering, in the model presented above (i.e., with those boundary conditions),

$$x_{1/2}\Big|_{\substack{\text{multiple}\\ \text{scat.}}} \simeq 1.12\,\frac{\theta_c^2}{2\sigma_s L_n n} = \frac{2.2}{\pi}\,\frac{\theta_c^2}{\psi_1^4 d^2 L_n n} \quad ,$$

where $L_n = \ln(1.29\epsilon)$, and ψ_1 and ϵ are defined by Lindhard.[7]

Since L_n is the order of 2–10 in the experiments described here, the dechanneling from interstitials in the planar case will be dominanted by multiple scattering.

For this effect to account for the total observed dechanneling rate would require an interstitial density of $\sim 4\times10^{20}$ defects/cm^3. It is interesting to note that this is the order of density of interstitials that can be determined from conventional channeling experiments; it might possibly be the case that the dechanneling is more sensitive a tool for observing self-interstitials than channeling.

The most abundant known impurity in these crystals has concentrations too low to give the required scattering even if it is assumed that all impurities are at interstitial sites; so one can conclude that interstitial impurities caused insignificant dechanneling in our case.

4. Electronic Interactions

Lindhard[7] has estimated the contribution to multiple scattering from electronic encounters. Using an average electron density of the solid, his estimate for electronic multiple scattering is $\sim\frac{1}{7}$ of the value of the normal multiple-Coulomb-scattering angle for silicon. There is significant evidence that a well-channeled particle sees an electron

density $\sim\frac{4}{14}$ of the average electron density in silicon.[14] Thus one may expect a scattering angle of 0.04 of the normal multiple-Coulomb-scattering angle. This contribution, though a factor of ~4 too small, approaches the angular deflection required to explain the experimental results.

As a proton passes through a solid it loses energy by single electron encounters and plasmon generation. The cross section for the plasmon type of energy-loss process is different than the single-electron encounters and hence leads to a different contribution to the multiple scattering of the incident ions. The plasmon contribution to the scattering is expected to be very small.

In order to obtain a better picture of the significance of the electron contribution to the multiple scattering and its importance relative to the nuclear contribution some simple estimates have been made, directed towards getting the applicable diffusion constants to complete the diffusion calculation. These estimates simply involve calculating the multiple scattering due to electronic or nuclear collisions while averaging over the ions planar channeling trajectory. In the electronic case this is carried out by forming the product of the electron density across the plane, calculated from the Lindhard average potential, and the probability distribution for continuum planar channeling given in Ref. 7 and integrating over the planar space. Thus,

$$\langle\theta^2\rangle_{t,e} = \frac{m}{2M_1E} S_e \int_{y_{\min}}^{y_{\max}} P(\theta,y)\rho(y)\,dy \ ,$$

where $\rho(y)$ is the electron-density distribution as a function of distance y from the planar wall and is taken as

$$-4\pi\rho(y) = \frac{\partial^2}{\partial y^2} Y(y) \ ,$$

where $Y(y)$ is the Lindhard planar potential. The probability of a particle with crossing angle θ being in the position y is given by

$$P(\theta,y) = \frac{c}{d_p}\left(\frac{E\theta^2}{E\theta^2 - Y(y)}\right)^{1/2} \ , \quad E\theta^2 > Y(y)$$

$$= 0 \ , \qquad\qquad E\theta^2 < Y(y)$$

where d_p is the planar spacing. In these equations m/M_1 is the ratio of electron to proton mass, E is the energy of the particle, and S_e is given by

$$S_e = (4\pi Z_1^2 e^4/mv^2)L_e \ ,$$

where $L_e \simeq \ln(2mv^2/I)$ and I is the average excitation potential.

The nuclear multiple scattering along the plane may be carried out in the same fashion although the mathematics is a good deal more difficult. Schiøtt[18] has carried out this nuclear calculation and the results for both electronic and nuclear cases for the case of 5.0-MeV protons in the {110} plane of silicon are shown in Fig. 15. Clearly the most striking feature of these curves is the dominance of the electronic contribution at small angles. A serious shortcoming of the nuclear contribution is the lack of inclusion of thermal vibrations. Thus a better indication of the nuclear multiple scattering may be from Barrett's[19] calculation which includes thermal vibrations and yields 1.4×10^{-4} deg$^2/\mu$m for the angular extent of the transmitted pattern, i.e., including all transverse energies. Even in this case, however, the electronic contribution dominates by a factor of 1.5 at the lowest transverse energies.

This calculation may be compared with the angular dispersion of the least-energy-loss particles discussed in Sec. III B. The measurement yielded a value of 2.3×10^{-3} deg$^2/\mu$m. If we estimate that a well-channeled particle stays at least 0.6 Å from the planar wall, such a particle has a crossing angle of 0.047 and the corresponding electronic contribution is given by Fig. 15 as 6×10^{-4} deg$^2/\mu$m, a factor of 4 lower than experiment.

Recent measurements by Altman[13] in a thin (~ 6.5-μm) Si crystal show the experimental angular spread reduced to 8.6×10^{-4} deg$^2/\mu$m, in better agreement with the calculation suggesting that there is some contribution from large transverse energies to the measured angular spread in

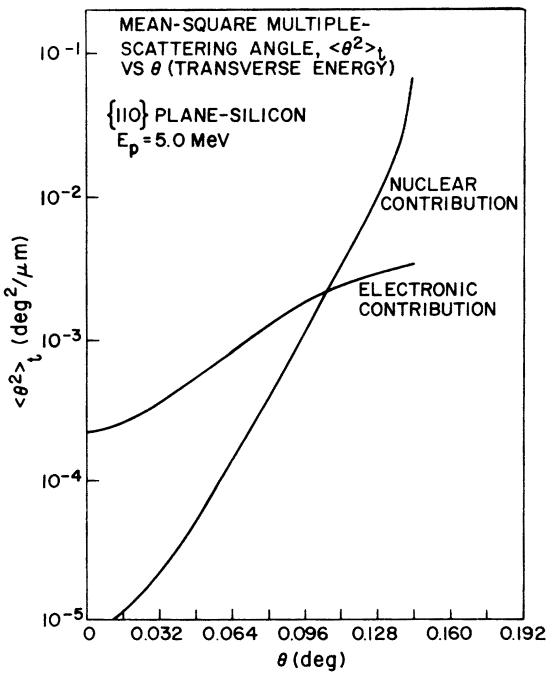

FIG. 15. Calculated multiple-scattering angle as a function of crossing angle.

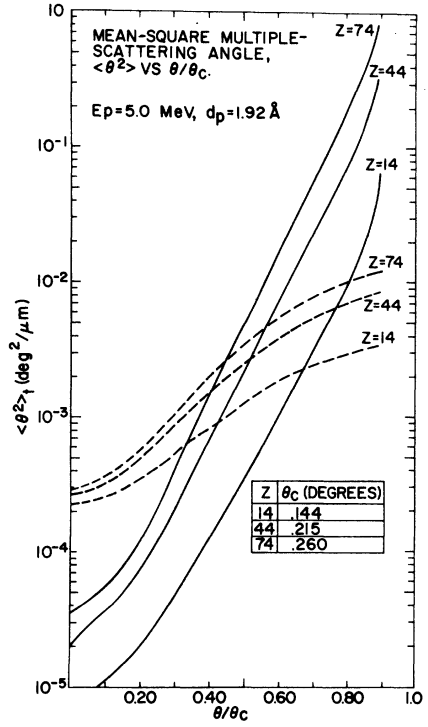

FIG. 16. Calculated multiple-scattering angle as a function of crossing angle for crystals of various atomic numbers.

the thick crystals.

It should be emphasized that we are not suggesting that only the electronic component is important, but that it is an important part of the total dechanneling mechanism.

Similar calculations of the multiple-scattering angle have been carried out for other materials as shown in Fig. 16. As expected, the contribution from the nulcear component becomes relatively more important for the higher-Z matérials and, when thermal vibrations are included, will probably dominate.

C. Transmitted Energy Spectra

On the basis of an exponential escape law it is possible to explain the total energy spectrum of protons transmitted through a thick silicon target in a channeling orientation. Figure 17 shows such a spectrum for a 47-μ silicon crystal with the beam parallel to the {111} plane (open circles). The large peak at 4.34 MeV corresponds to the "normal energy" while the small peak at 4.68 MeV is interpreted as due to particles that have stayed in the channel throughout the thickness of the crystal. The large number of particles with energies between these two peaks may be interpreted as those that have escaped the channel at some thickness and thus have an energy loss intermediate between the normal peak and entirely channeled peak. Using the following measured parameters: dispersion of the detector system, normal energy loss, channeling energy loss, straggling in the normal and channeling energy loss, and the half-thickness, together with the theoretical percentage of particles initially normal from the Lindhard model and Eq. (16), we have simulated the measured energy spectrum. The simulation (closed dots) is compared to experiment (open dots) in Fig. 7 and indicates good agreement with most of the characteristics of the measured spectrum.

V. CONCLUSIONS

A. Exponential Escape

As discussed in Sec. III A1, the transmitted particle energy spectrum is a very direct reflection of the escape rate when assuming the simple two-energy-loss model. Within this model the constant decay rate, characteristic of an exponential decay, is clearly the best fit to the data. In some cases the exponential decay is observed over 3–5 half-thicknesses, a range much greater than may be observed practically in most backscattering experiments.

However, one must recognize that the two-energy-loss model is an over simplified picture. It

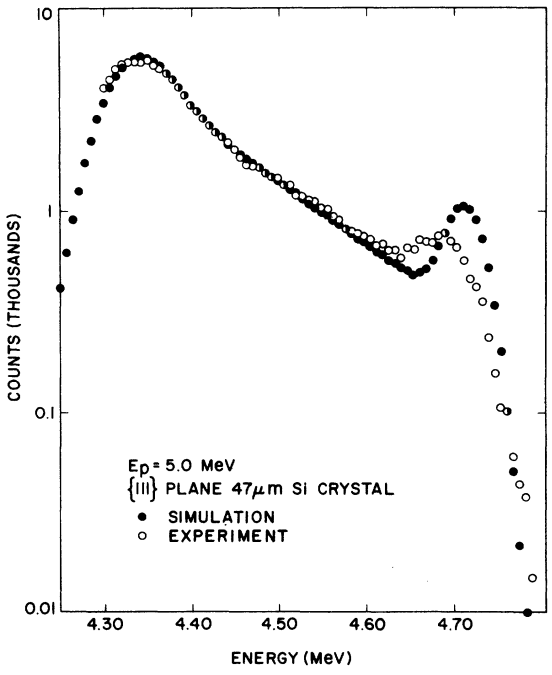

FIG. 17. Comparison of the measured energy distribution of 5.0-MeV protons transmitted through a 47-μ Si crystal in the {111} direction (open circles) to a simulated spectrum (closed circles) which uses various measured parameters.

is clear that even in the absence of particle escape the emergent particle distribution would contain a complete continuum of energies from E_C to E_R and below. Such a distribution in fact would have a maximum intensity at E_C and decrease to a minimum near E_R, i.e., a slope of oppostie sign to the observed spectrum. This effect, if properly subtracted, would tend to decrease the observed half-thicknesses and increase the difference between the backscattering results of $x_{1/2}$ and the transmitted results of $x_{1/2}$.

Qualitatively one might expect this correction to be small. Initially all angles are populated with the distribution peaking at 0°. Those particles with small crossing angles will diffuse very slowly as shown in Fig. 16 while those with larger transverse energies diffuse out of the channel rapidly, the large nuclear-multiple-scattering dominating for larger transverse energies. Thus it is easy to imagine that any one particle spends a relatively short time in the high-transverse-energy intermediate-energy-loss region during its total transit time through the crystal. If the measured half-thickness is the order of 10 μm for 0° incidence, the half-thickness for the larger transverse energy must be substantially smaller and in these transmission experiments in which 30–50-μm crystals were used the contribution to the emergent energy from its time in the high-transverse-energy region must also be small. More detailed calculations will be required before this effect can be put on a more quantitative basis.

The initially flat portion of the depth profile of the channeled beam observed in Ref. 2 by backscattering is probably due to the high scattering yield of the "hard component" making the channeled fraction appear lower, the effect diminishing in a rather short thickness since the multiple scattering of this component is large. As would be expected on the basis of this explanation, this effect would not be observed as a flattening in the escape portion of the transmitted energy distributions but would show up as a peak or broadening on the low-energy side of the spectrum. Because of the large number of "normal" energy-loss particles present and the small number of hard component particles expected such an effect is difficult to detect.

B. Comparison of Methods of Obtaining $x_{1/2}$

We have found that the characteristic thickness parameter for dechanneling is approximately the same when measured in the transmission mode or the backscattering mode. When using the minimum value of channeling energy loss in both analyses the transmission results are about 10% lower than the backscattering results. This may be a result of the different observables in these two techniques. It is possible that "escape to normal energy loss" occurs faster than "escape to normal backscattering yield."

C. Choice of Channeled Energy Loss

As has been shown by other authors and also in Eq. (15) the correction for the lower energy loss of the channeled incident particle in the backscattering technique represents a relatively small uncertainty in the extracted value of $x_{1/2}$. The transmission method, on the other hand, is very sensitive to the chosen value of R and this adds an additional uncertainty. We have found that the two methods agree when R is close to but slightly larger than the observed minimum value. This result comes about primarily because of their relative sensitivities.

The resonance experiment described in Sec. III A2 allows an upper limit of $R\{110\}=0.87$ and $R\{111\}=0.81$; the lower limits correspond to $R\{110\}=0.6$ and $R\{111\}=0.44$. These two extremes represent a factor of 2.3 in the extracted $x_{1/2}$ value by transmission.

D. Energy Dependence of $x_{1/2}$

The linear dependence of $x_{1/2}$ with E is borne out for a large range of energies in both the backscattering results and the transmission results. This is to be expected for almost any type of multiple-scattering process. The fact that the curves do not go through the origin may be explained by noting the log term in the multiple-scattering formula. For example, Lindhard[7] shows that the multiple scattering for electrons is given by

$$\langle\theta^2\rangle_e \propto \ln(kE)/E$$

in which, in the random case, $k=4m/MI_0Z_2$, where I_0 is the order of 10 eV. In the random case the log term begins to be important at ~2 MeV. It is not clear what value of k to use in the channeling case; however, it is most probably smaller than the random value and thus would lead to deviation from linearity in $x_{1/2}$ at energies ≤ 2 MeV. It is worth noting that this log term may be important in extrapolating results to other energies and materials.

E. Multiple-Scattering Measurements

The measurements of the proton intensity distribution along the plane are approximately Gaussian giving strong evidence for the multiple-scattering argument. In magnitude they are one-tenth of the multiple-Coulomb-scattering angles measured in a sample of the same thickness but of amorphous structure. The energy dependence is the same as for normal multiple Coulomb scattering and most probably indicates a Coulomb-scattering process. The comparison with the calculated values indicates that the electronic mul-

tiple-scattering contribution is probably the limiting mechanism in this diffusion effect, although the estimates indicate that the nuclear contribution is not negligible.

The extracted values of $x_{1/2}$ using Eq. (18) and the experimental parameters for ψ_c and $\langle\theta^2\rangle_t^{1/2}$ are a factor of ~3 smaller in Si and a factor of ~2 smaller in Ge than experiment. This difference may result from assumption that the multiple scattering along the plane is the same as across the plane. This would appear to be a reasonable assumption for electronic multiple scattering but not nuclear multiple scattering.

Further, a more sophisticated treatment of the diffusion model with a variable diffusion coefficient, and inclusion of effects due to such processes as "rechanneling" of the random beam would tend to increase the theoretical values of $x_{1/2}$.

There is also some indication that the measurement of $\langle\theta^2\rangle_t$ depends on crystal thickness, crystals the order of $x_{1/2}$ giving values of $\langle\theta^2\rangle_t$ approximately one-half of the results presented here. This is probably due to an increase in the population of large transverse energies.

It is interesting to note that the ratio of $\langle\theta^2\rangle_t$ for Ge to $\langle\theta^2\rangle_t$ for Si is almost one, while normal nuclear multiple scattering would predict a factor of ~2. If the electron density in the center of the channel is the same for both Ge and Si and if electronic scattering is dominant, then one would expect the observed ratio.

ACKNOWLEDGMENTS

The authors are happy to acknowledge many useful and stimulating discussions with W. L. Brown. They are grateful to H. Schiøtt for the use of his results before publication. M. R. Altman and J. Hirvonen aided in taking some of the data for which we are thankful and T. C. Madden employed his usual expertise in the preparation of the single crystals. The higher-energy work was done on the Rutgers-Bell tandem. The cooperation of the personnel of that installation is gratefully acknowledged. We have profited from useful discussion with our colleagues J. U. Andersen, J. H. Barrett, W. M. Gibson, M. T. Robinson, and H. Schiøtt.

[1]L. C. Feldman, Ph.D. thesis (Rutgers University, New Brunswick, N. J., 1967) (unpublished).
[2]J. A. Davies, J. Denhartog, and J. L. Whitton, Phys. Rev. 165, 345 (1968).
[3]S. T. Picraux and J. U. Andersen, Phys. Rev. 186, 267 (1969).
[4]B. R. Appleton, L. C. Feldman, and W. L. Brown, Brookhaven National Laboratory Report No. BNL 50083 C52, p. 45 (unpublished).
[5]L. C. Feldman, B. R. Appleton, and W. L. Brown, in Ref. 4, p. 58.
[6]J. U. Andersen, J. A. Davies, K. O. Nielsen, and S. L. Andersen, Nucl. Instrum. Methods 38, 210 (1965).
[7]J. Lindhard, K. Dan. Vidensk. Selsk. Mat.-Fys. Medd. 34, No. 14 (1965).
[8]M. W. Thompson, in Ref. 4, p. 106.
[9]G. Dearnaley, I. V. Mitchell, R. S. Nelson, B. W. Farmery, and M. W. Thompson, Philos. Mag. 18, 985 (1968).
[10]F. Abel, G. Amsel, M. Bruneaux, and E. D'Artemare, J. Phys. Chem. Solids 30, 687 (1969).
[11]G. Foti, F. Grasso, R. Quattrocchi, I. F. Quercia, and E. Rimini, Nuovo Cimento Lett. 15, 707 (1970); S. U. Campisano, F. Grasso, and E. Rimini, Radiat. Eff. 9, 153 (1971); S. U. Campisano, G. Foti, F. Grasso, and E. Rimini, Phys. Lett. A 35, 119 (1971).
[12]K. Morita and N. Itoh, Phys. Lett. A 31, 283 (1970).
[13]M. R. Altman, Ph.D. thesis (Rutgers University, New Brunswick, N. J., 1969) (unpublished).
[14]B. R. Appleton, C. Erginsoy, and W. M. Gibson, Phys. Rev. 161, 330 (1967).
[15]S. Datz, C. D. Moak, T. S. Noggle, B. R. Appleton, and H. O. Lutz, Phys. Rev. 179, 315 (1969).
[16]R. M. Sternheimer, Phys. Rev. 115, 137 (1959).
[17]M. R. Altman, L. C. Feldman, and W. M. Gibson, Phys. Rev. Lett. 24, 464 (1970).
[18]H. Schiøtt (private communication).
[19]J. H. Barrett, Phys. Rev. B 3, 1527 (1971).